

Endohedrally confined hydrogen atom with a moving nucleus

This content has been downloaded from IOPscience. Please scroll down to see the full text.

2016 J. Phys. B: At. Mol. Opt. Phys. 49 235003

(<http://iopscience.iop.org/0953-4075/49/23/235003>)

View [the table of contents for this issue](#), or go to the [journal homepage](#) for more

Download details:

IP Address: 168.96.255.109

This content was downloaded on 02/02/2017 at 14:17

Please note that [terms and conditions apply](#).

You may also be interested in:

[Quantum Chemistry: The hydrogen atom](#)

A J Thakkar

[Energy-level structure of the hydrogen atom confined by a penetrable cylindrical cavity](#)

R Cabrera-Trujillo, R Méndez-Fragoso and S A Cruz

[Confinement effects on the electron transfer cross section: a study of He²⁺ colliding on atomic H](#)

R Cabrera-Trujillo

[Sturmian bases for two-electron systems in hyperspherical coordinates](#)

A Abdouraman, A L Frapiccini, A Hamido et al.

[Polarizability of off-center spherically confined hydrogen atom](#)

R L Melingui Melono, A J Etindélé, T Tchakoua et al.

[Multi configurational explicitly correlated wave functions for the study of confined many electron atoms](#)

A Sarsa, E Buendía and F J Gálvez

[Electric response of endohedrally confined hydrogen atoms](#)

S A Ndengué and O Motapon

[Wave packet simulations of antiproton scattering on molecular hydrogen](#)

Henrik Stegeby, Markus Kowalewski, Konrad Piszczatowski et al.

[Precise estimation of the energy levels of two-electron atoms under spherical confinement](#)

S Bhattacharyya, J K Saha, P K Mukherjee et al.

Endohedrally confined hydrogen atom with a moving nucleus

J M Randazzo and C A Rios

División de Colisiones Atómicas, Centro Atómico Bariloche and CONICET, 8400 San Carlos de Bariloche, Río Negro, Argentina

E-mail: randazzo@cab.cnea.gov.ar

Received 19 July 2016, revised 26 September 2016

Accepted for publication 10 October 2016

Published 16 November 2016



CrossMark

Abstract

We studied the hydrogen atom as a system of two quantum particles in different confinement conditions; a spherical-impenetrable-wall cavity and a fullerene molecule cage. The motion refers to the center of spherical cavities and the Schrödinger equation is solved by means of a generalized Sturmian function expansion in spherical coordinates. The solutions present different properties from the ones described by the many models found in the literature, where the proton is fixed in space and only the electron is considered as a quantum particle. Our results show that the position of the proton (i.e. the center of mass of the H atom) is very sensitive to the confinement condition, and could vary substantially from one state to another, from being sharply centered to being localized outside the fullerene molecule. Interchange of the localization characteristics between the states when varying the strength of the fullerene cage and mass occurred through crossing phenomena.

Keywords: confined atoms, fullerene, hydrogen

(Some figures may appear in colour only in the online journal)

1. Introduction

Being the simplest atomic system, hydrogen is one of the most extensively studied elements in the periodic table. The atom has a relatively simple mathematical description through the analytical solution of the two-body Schrödinger equation, which enables comprehension of its electronic structure, its quantum states, its discrete nature of energy levels, and other related properties. From the experimental side, it has been bombarded with electrons [1], protons [2, 3] and photons [4, 5], combined with other chemical elements and, more recently [6, 7], confined in fullerene structures.

The wave functions which theoretically describe these processes are usually obtained from the hydrogen-like Schrödinger equation, by considering separately the center of mass and relative coordinates [8]. The problem maps to a central field problem for a reduced mass μ particle, and since μ is very similar to the electron mass, it is usually interpreted as if it were the electron, and the nucleus were fixed at the center of the coordinate system. The quantum behavior of the center of mass is not generally considered, since the interesting properties, such as ionization energies or the excited

state structure, only depend on the relative coordinate dynamics.

The same approach is sometimes applied when atomic confinement is modeled [9–12], where the proton is generally considered as an infinitely massive particle fixed in space, acting as a Coulomb center for the electrons clamped somewhere in the box [13, 14]. In the case where the proton is not centered, the separation of coordinates is not possible, as discussed by Tanner [15] and Amore (and Fernández) [16] for a harmonic oscillator. The way to deal with such a system while keeping two-body simplicity is to consider the electron-wall interactions of a spherical box or fullerene molecule through boundary conditions [17] or central potentials [18] respectively, as a function of the radial coordinates. The movement of the nucleus can then be considered perturbatively [13], or in the Born–Oppenheimer approximation, where the energy value of the system as a function of its coordinates defines a potential energy surface (PES) through which it moves [19].

An alternative way is to consider the system as a three-body problem, consisting of a proton, an electron and a confinement cavity. A first approximation to the ground state

solution of the hydrogen atom in an infinitely massive spherical box was introduced by Fernández [20], who performed a variational calculation with a very simple trial function, which seems to be adequate for strong confinement, i.e. R_c (radius cage) < 1 a.u. Better results have been found in a more recent calculation with a generalized Hylleraas basis set of four linear parameters and three exponentials [21], where mean values of some observables were given for the ground state as a function of the confinement radius.

In this work we extend the study of the confined hydrogen atom with a moving nucleus to the case of endohedral confinement. We emphasize the analysis to the localization of the proton, identifying the confinement conditions which are (and are not) compatible with the usual atom-centered models. The solution of the Schrödinger equation is obtained by means of a configuration interaction (CI) approach with generalized Sturmian functions, in the coordinates which locate the proton and electron from the center of the confinement cage.

The paper is organized as follows: in section 2 we introduce the driven equations for the system and the mathematical tools we used to solve them. In section 3 we show convergence of the calculations. We present results for the ground state of the hydrogen atom and describe localization phenomena of the atom for some confinement conditions. The finite mass of the confinement molecule and crossing phenomena between the states as a function of the interactions strength and molecular mass is described. Finally, a summary and some concluding remarks are given in section 4. Hartree atomic units ($\hbar = m_e = e = 1$) are used throughout this paper.

2. Theory

We consider the confined hydrogen atom as a system of two quantum particles inside a spherical cage of radius R_c , where the center of the sphere is considered as the center of the coordinate system. The Hamiltonian can be written as:

$$H = -\frac{\nabla_e^2}{2\mu_e} - \frac{\nabla_p^2}{2\mu_p} - \frac{1}{m_c} \nabla_e \cdot \nabla_p + U_e(r_e) + U_p(r_p) - \frac{\lambda}{r_{ep}} \quad (1)$$

where the sub-index e (p) denotes the relative coordinate and reduced mass associated to the electron (proton)-cage pair, where m_c is the mass of the cavity and r_{ep} is the electron-proton distance, while λ is the strength of the interaction (i.e. $\lambda = 1$ for hydrogen). We study two cases, the particles inside a spherical box with impenetrable walls, and a model of endohedral fullerene confinement. In the first case, we take $U_e = U_p = 0$ and impose the boundary condition $\Psi(\mathbf{r}_e, \mathbf{r}_p) = 0$ for r_e or r_p equal or greater than R_c . Also we considered $1/m_c = 0$ which corresponds to infinite m_c .

In the second case, the confinement is associated with a fullerene cage considered to be finite or infinitely massive ($m_c \simeq 720$ times m_p). For the electronic potential we use the

well given by Connerade *et al* [18]:

$$U_e(r) = \begin{cases} -U_0 & 0 < r \leq r_c + \Delta \\ 0 & \text{otherwise} \end{cases} \quad (2)$$

where r_c and Δ are the inner radius and the thickness of the shell, respectively. We use the values deduced by Xu *et al* [22] ($r_c = 5.75$ a.u. and $\Delta = 1.89$ a.u.), which are specific for a C_{60} molecule. On the other hand, the value of U_0 is changed in order to explore the general physics of the system. In a physical picture, this value can actually be changed; for example modifying the number of atoms of the molecule and therefore the fullerene structure. Within this model, m_c can take finite values as we show in the results.

It follows that the complex physics involved in the chemical processes for $H - C_{60}$ are not included in this model. Indeed, the interaction of the proton with the fullerene cage should be different from U_e because of the different physical properties, principally its mass, charge and indistinguishability with other constituent particles of the molecule. However, since the proton has the opposite electron's charge, it is naturally suggested to consider, as a first approximation to more elaborate models, the choice $U_p(r) = -U_e(r)$. This election also takes into account, on average, the H-C repulsive core effect at short distances, typical of inter-atomic potentials. On the other side, the active electron bounded to the well acts as an attractive potential for the proton at large distances, through the Coulombic interaction. Independently of the veracity of the proposed interaction, the present model will allow us to discover and understand some interesting properties of the collective quantum dynamics of two particles with quite different masses.

2.1. Sturmian expansion

In order to have a spatial representation of the eigenstates we use the Sturmian basis, which satisfies the equation:

$$\left[-\frac{1}{2m_i} \nabla_{\mathbf{r}_i}^2 + U_i(r_i) - E_i \right] \Psi_{\nu_i}(\mathbf{r}_i) = -\beta_{\nu_i} V(r_i) \Psi_{\nu_i}(\mathbf{r}_i), \quad (3)$$

together with the physical boundary conditions:

$$\int |\Psi_{\nu_i}(\mathbf{r}_i)| d\mathbf{r}_i^3 < \infty \quad (4)$$

$$\Psi_{\nu_i}(\mathbf{r}_i) = 0 \text{ for } r_i = R_c, \quad (5)$$

where $r_i = |\mathbf{r}_i|$, $\nu_i = \{n_i, l_i, m_i\}$ and $i = e, p$.

The Sturmian basis results from (3) and the conditions (4) and (5), by taking the energy E as an externally fixed parameter and β_{ν} as the eigenvalue to be determined (here ν stands for all quantum numbers) [23]. V is any atomic-type potential which depends only on the distance r_i and satisfies $V(r_i) = 0$ for $r_i > R_c$.

Equation (3) is separable in spherical coordinates as usual:

$$\Psi_{\nu_i}(\mathbf{r}_i) = \frac{1}{r_i} P_{n_i, l_i}(r_i) Y_{l_i, m_i}(\theta_i, \varphi_i), \quad (6)$$

and we only have to solve for $P_{n_i, l_i}(r_i)$:

$$[T_{r_i} + U_i(r_i) - E_i] P_{n_i, l_i}(r_i) = -\beta_{\nu_i} V(r_i) P_{n_i, l_i}(r_i) \quad (7)$$

where T_r is the radial kinetic energy operator:

$$T_r = -\frac{1}{2m} \frac{d^2}{dr^2} + \frac{l(l+1)}{2mr^2}. \quad (8)$$

The boundary condition (4) ensures the regularity of the Sturmian functions, while the boundary condition (5) depicts the confinement. For the spherical box case, R_c is the radius of the cage; while for endohedral fullerene confinement it is chosen to be large enough to affect negligibly the wave functions which are localized by the fullerene potential.

As is usual in uncorrelated CI calculations, we use a partial-wave expansion for the Coulomb interaction:

$$\frac{\lambda}{r_{ep}} = \lambda \sum_{l=0}^{\infty} \frac{r_{<}^l}{r_{>}^{l+1}} \frac{4\pi}{2l+1} \sum_{m=-l}^l Y_l^m(\hat{\mathbf{r}}_e) Y_l^{m*}(\hat{\mathbf{r}}_p), \quad (9)$$

where $r_{>}$ ($r_{<}$) is the greater (smaller) between r_e and r_p . The eigenfunctions of the Hamiltonian given by equation (1) can be written as:

$$\Psi^{L,M}(\mathbf{r}_e, \mathbf{r}_p) = \sum_{\nu} a_{\nu}^{L,M} \Phi_{\nu}^{L,M}(\mathbf{r}_e, \mathbf{r}_p), \quad (10)$$

where

$$\Phi_{\nu}^{L,M}(\mathbf{r}_e, \mathbf{r}_p) = \frac{P_{n_e, l_e}(r_e)}{r_e} \frac{P_{n_p, l_p}(r_p)}{r_p} \mathcal{Y}_{l_e, l_p}^{L,M}(\hat{\mathbf{r}}_e, \hat{\mathbf{r}}_p) \quad (11)$$

and $\nu = \{l_e, l_p, n_e, n_p\}$. Note that we use the spherical bi-harmonics $\mathcal{Y}_{l_e, l_p}^{L,M}$, which are eigenfunctions of the total angular momentum operator and its projection along the \hat{z} axis with quantum numbers L and M respectively.

By means of the Galerking method and standard algebra packages [24] we obtain solutions for the coefficients $a_{\nu}^{L,M}$ and eigenenergies E [23].

3. Results

3.1. Convergence properties of the expansion

The convergence of the wave functions with the number of radial configurations included in the expansion can be analyzed through the ground-state energy. Here we consider the hydrogen atom ($U_0 = 0$) in a spherical box of radius $R_c = 10$ a.u., as a function of the radial basis elements per coordinate. Since partial wave convergence will be analyzed later, here we restrict our study to the $l_e = l_p = 0$ component, corresponding to the $L = 0$ partial-wave term. We will use two basis sets. One is the box-based Sturmians SF_b (i.e. $U_i = 0$ and $V_i = 1$, $i = e, p$) which depend only on the value of R_c , the distance at which homogeneous conditions are imposed. This is the basis we will use in the next section, where the depth of the potential U_0 and the Coulomb interaction strength λ will be varied.

Before we present our results, we would like to stress that the Sturmian functions can be defined to efficiently represent a particular state [23]. In order to show this, we propose as an example a second basis which gives better results with smaller basis elements than the SF_b . This optimal basis SF_o is

Table 1. Convergence analysis for the $l_e = l_p = 0$ ground state of the confined hydrogen atom as a function of radial functions per particle n_{\max} with the box based (SF_b) and ‘sophisticated’ (SF_o) radial Sturmians.

n_{\max}	Ground-state energy	
	SF_b	SF_o
5	-0.2905806409	-0.4470251209
10	-0.3729047660	-0.4663337297
15	-0.4130974121	-0.4672219778
20	-0.4353883725	-0.4672434215
25	-0.4485486681	-0.4672446242
30	-0.4565116034	-0.4672448546
35	-0.4613104686	-0.4672448585
40	-0.4641220711	-0.4672449074
45	-0.4656910723	-0.4672448904
50	-0.4665127698	-0.4672449113

defined through $U_i = 0$, $V_i = r_i^{-1} e^{-\alpha_i r_i}$ ($i = e, p$), $E_e = E_p = -0.5$ and $\alpha_p = 2\alpha_e = 1$ in equation (3). The potentials and parameters we have just defined were chosen based in our previous experience [23] and performing few variational iterations. A deeper optimization can also be performed in all parameters and functional space of potentials V_i .

In table 1 we show the ground state energies of the s-wave ($l_e = l_p = 0$) confined H atom as a function of the number of radial states per coordinate. In this analysis we use $R_c = 10$ a. u. in order to have acceptable convergence with small SF_b basis sets. For the results of the next sections we set $R_c = 20$ a. u. in order to reduce effect of the confinement at large distances on the evaluated states. We have checked that the spatial distribution of the states for larger values of R_c remain mainly unchanged. We clearly see that the optimized basis is much more efficient than the unoptimized one. However, the disadvantage of optimization is that it has to be performed for each individual state in an iterative procedure. Here we reach, with the SF_o , convergence of the radial expansion for the ground state of the system until the 6th decimal figure by using 25 radial functions per coordinate, while for the same size the SF_b basis gives only up to the first one.

Deeper values of the energy can be obtained by adding angular terms. This is done through bi-spherical harmonics, in the same fashion as for the SF_b and SF_o basis sets. The expected energy for the ground state will be close to -0.5 , which is a little bit higher due to the finite size of the basis and the confinement effects. If we were dealing with a H atom modeled as a single neutral particle in a box, the amount of the total energy associated with the confinement effect would be $\pi^2/2R_c^2(m_e + m_p) \simeq 2.7 \times 10^{-5}$, i.e., the exact ground-state energy of the system. However, as we will see, the true state corresponding to a two-particle wave function is very different in shape if we look at the center-of-mass distribution, which almost equals the proton’s distribution. That is why we cannot estimate *a priori* the confinement energy of the composed system.

Table 2. Convergence analysis for ground state of the confined hydrogen atom as a function of the maximum number of partial waves (l_{\max}) added when using 20 radial functions per coordinate, with the box based (SF_b) and ‘sophisticated’ (SF_o) radial Sturmians.

l_{\max}	Ground-state energy	
	SF_b	SF_o
0	-0.4353883725	-0.4672434215
1	-0.4748432442	-0.4878532032
2	-0.4843652580	-0.4922149011
3	-0.4884665735	-0.4934791747
4	-0.4907433951	-0.4939416245
5	-0.4921976351	-0.4941458680
6	-0.4932104410	-0.4942489924
7	-0.4939553268	-0.4943062823

In table 2 we show the energy values of the ground state energy of the system as a function of the maximum number of pairs (l_e, l_p) for the s-wave solution ($l_e = l_p$), when the number of radial functions per coordinate is 20 (note that the values for $l_{\max} = 0$ are the same as the value for $n_{\max} = 20$) in table 1. We clearly see an improvement in the energy value when increasing l_{\max} .

As we are not introducing the relative coordinate r_{ep} in our expansion, the convergence of the energy is much less efficient than in the case of the generalized Hylleraas series, since with fewer basis functions, the Hylleraas expansion gives better results. Moreover, if one considered the spherical coordinates we use, the Kato cusp conditions [25] would be found in the angular coordinates. This sharp behavior cannot be reached with spherical harmonics. However, the CI calculation with a large number of configurations is more complete, in the sense that a great variety of distributions can be described with it. In fact, the eigenvalue calculation which gives the last element of table 2 corresponds to an expansion with $20 \times 20 \times (7 + 1) = 3200$ basis elements, which gives rise to the same number of eigenstates. In our case we do not know the distribution we are going to find, so the basis must be general and not optimized for hydrogenic states.

3.2. Ground state 1S: spatial distribution

Let us now study how the confinement influences the wave functions, and determine the particle’s spatial distribution. Starting with the spherical box considered in the previous section, we vary the interaction between the particles through the λ parameter (shown in equation (1)) and the strength U_0 that describes the interaction with the fullerene cage, taking into account only s-wave partial wave terms. The results are summarized in figure 1.

The first solution is obtained by setting $\lambda = U_0 = 0$ (top left), and corresponds to the box-based behavior in each coordinate. The uncorrelated Hamiltonian is separable in spherical coordinates, the solution is exact and can be described by a single product of Sturmian functions. When the C_{60} potential model is turned on to $U_0 = 1$ ($\lambda = 0$) (top right), the electron moves to the well while the proton, which

sees a repulsive barrier, stays in the external region. It is still contained by the walls at R_c , but if an infinite radial domain were used, its spatial distribution would be that of an unbounded particle. If the Coulomb potential is turned on in the absence of the fullerene well, ($\lambda = 1$ and $U_0 = 0$), both particles get close to the center of the sphere, as is shown in the bottom-left part of figure (1). This appears to be a strange behavior, since the global H system is neutral, and it would be expected the distribution of a particle of mass $m_e + m_p$ inside a spherical well for the center of mass of the H atom, which is practically coincident with the proton position. Instead, we find a very sharp wave function; a product of the interaction of the complex two-particle system with the boundary. In order to understand this behavior, we have to take into account that the proton is much heavier than the electron, and its confinement is less expensive from an energetic standpoint.

Since the ground state lacks nodal curves [26] and must be null at the surface of the confining sphere, we supposed that the wave function would be a decreasing function of the electronic coordinate, having its maximum at the center of the sphere. This is true for small R_c , where confinement energy becomes more important than Coulomb interaction [27]. Such distribution would act as a potential energy surface (PES) for the proton, giving a distribution centered at its minimum (the maximum of the electronic distribution) with a very small width because of its mass. Now we can argue that the electronic distribution of this particular state would be the one that adjusts to a proton located at the center of the coordinates [9, 10, 15, 17], as many models established. We have increased the value of the cage radius up to $R_c \simeq 100$ a.u. and found the same centered distribution.

The plot of the bottom-right part of figure 1 corresponds to the ground state of two interacting Coulomb particles in the presence of the C_{60} potential ($\lambda = 1$ and $U_0 = 1$). In this case the wave function describes the electron in the well while the proton, attracted by the electron and repelled by the potential, is located in the internal part of the fullerene cage. This result shows a significant difference with the models of endohedral confinement with the centered atom.

3.3. Behavior of the spectrum

To deepen the understanding of the results, let us analyze the energy spectrum for different values of U_0 , with and without Coulomb interaction. Several of these statements are conclusions drawn from the analysis of both spectra graphs as several charts of wave functions for different conditions, analogous to those shown in figure 1.

The energies are shown in figure 2, where we plot them in increasing order for the s-wave model ($l_e = l_p = 0$) in a calculation with 50 radial functions per coordinate, making a total of 2500 states. Here we use box based Sturmians ($U_i = 0$ and $V_i = 1$, $i = 1, 2$ and $R_C = 20$ in (7)), so that all uncorrelated calculations ($\lambda = 0$) are exact solutions. These are represented with black circles, and their values, obtained from

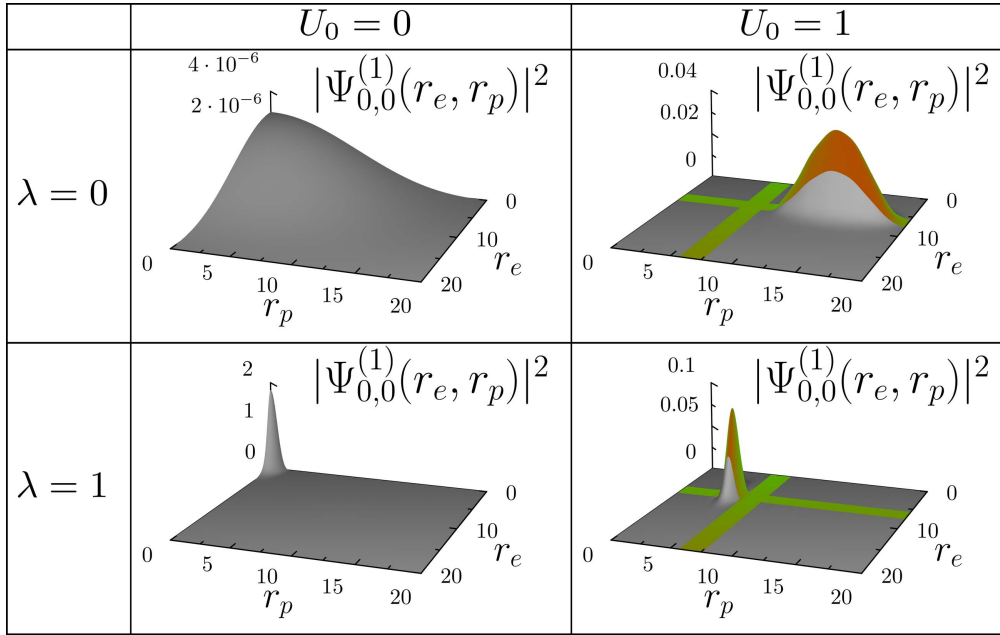


Figure 1. Spatial distributions of the ground states of the e-p system under different confinement conditions which are simulated by varying the strength of the interactions through the values of λ and U_0 (see text).

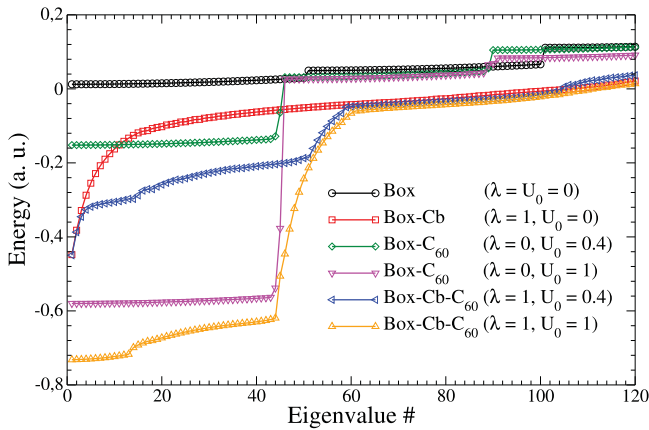


Figure 2. Energy value versus its order of appearance for the e-p system under various confinement conditions. Box conditions are imposed at $R_c = 20$ and two parameters describe the Coulomb (Cb) and the fullerene potential (C_{60}) interactions. (Black) circles: $\lambda = U_0 = 0$; (red) squares: $\lambda = 1$ and $U_0 = 0$; (green) diamonds: $\lambda = 0$ and $U_0 = 1$; (magenta) down triangles: $\lambda = 0$ and $U_0 = 1$; (blue) up triangles: $\lambda = 1$ and $U_0 = 0.4$; (orange) left triangles: $\lambda = 1$ and $U_0 = 1$.

the calculation, can also be determined by the expression:

$$E = E_p + E_e = (\pi n_e)^2 / 2R_c^2 m_e + (\pi n_p)^2 / 2R_c^2 m_p, \quad (12)$$

the ground state having energy equal to $E = 0.012343$ a.u. and corresponds to $n_e = n_p = 1$. These energies are obtained just by adding the energies of two non-interacting particles of masses m_e and m_p confined in an impenetrable spherical box.

The first 50 states correspond to the case $n_e = 1$ and $n_p = 1, 2, \dots, 50$, the small difference between them being a consequence of the mass value of the proton. A jump appears at the state number 51, which corresponds to the case ($n_e = 2, n_p = 1$), followed by the ($n_e = 2, n_p = 2, 3, \dots, 50$)

states, and so on. We must clarify that the jump between the $n_e = 1$ and $n_e = 2$ would be unnoticed if a minimum number of proton states were included such that $n_p \geq \sqrt{3m_p/m_e} \simeq 73$, which follows from equation (12).

A similar structure appears when correlation or other values of U_0 are considered. Coulomb interaction (red squares) with $U_0 = 0$ changes the nodal structure, laying the ($n_e = 2, n_p = 1$) state of energy -0.118891 a.u. in the 15th place (instead of the 51th) and moving down the whole set of values, the jump being now unobserved. For higher energies the Coulomb interaction becomes relatively less important than the confinement, and the slope of the curve (actually, a quadratic behavior) tends to that of the uncorrelated case. The ground-state energy is -0.447973 a.u., which is close to the ground state of the free hydrogen system.

With $\lambda = 0$ and $U_0 = 0.4$ (dark green triangle down), the first energy values are lower than for the $U_0 = 0$ case. On the one hand, this behavior is in accordance with the attractive effect of the C_{60} potential on the electron. On the other hand, it is repulsive for the proton and the effect should be the contrary. As we mentioned, the proton localization, in this case outside the repulsive barrier, is less expensive from an energetic point of view, while the bound energy of the electron in the well dominates. The $n_e = 1 \rightarrow 2$ ‘jump’ occurs now between the 44th and 46th places, with the 45th eigenvalue in a transition region, and corresponds to electron states which are bound for $n_e = 1$ and unbound for $n_e = 2$. The same happens with $U_0 = 1$ (magenta diamonds), with a bigger jump, since the effect of the potential is higher, still having only one electron bound state.

When $\lambda = 1$ and $U_0 = 0.4$ (blue triangle left), it corresponds to the confined H@ C_{60} model. The ordered energies present a structure which seems to be an admixture of the ones discussed above. We see that the energies of the first and

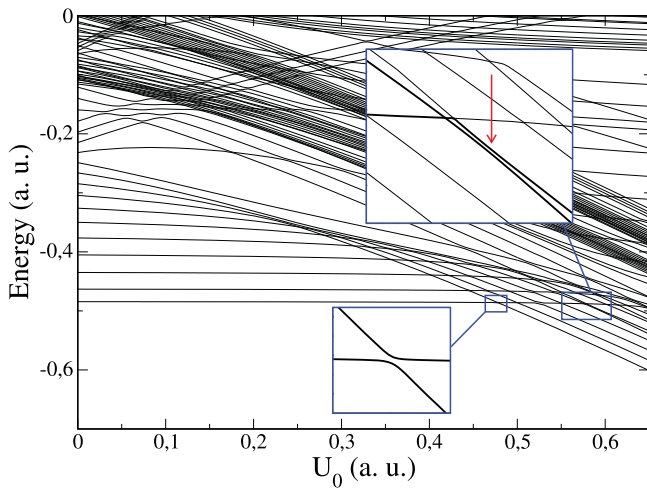


Figure 3. Evolution of the negative energy levels of the confined hydrogen atom as a function of U_0 .

second states are practically unchanged from the $U_0 = 0$ case. This is because the wave function is centered and without overlapping the well. The Coulomb structure breaks, and they follow states with the electron bounded to the well and the proton inside and outside it. The 50th to 59th states mostly have distributions in which the electron–proton pair is bounded and ‘glued’ to the surface from the inner side, while in the 60th both particles are outside the fullerene. For $\lambda = U_0 = 1$ (orange upwards triangle) the structure is similar, with a Coulomb structure (from state 44th to 60th) and lower ground state. In this case the ground-state energy is lower than -0.5 a.u., corresponding to the situation where the electron is in the well (lower right of figure 1). There exists, however, a state with energy -0.446197 a.u. which has almost the same probability distribution as the ground state for $U_0 = 0$. This state is in the 46th place, and consequently has a complex (hidden) nodal structure which is not present in the ground state for $U_0 = 0$.

The interchange of properties in the probabilities between different eigenstates when a parameter of the equation is changed, is related to what is called *crossings* of energies, and will be discussed in the next section.

3.4. Crossing phenomena

The behavior of the electronic energy levels as a function of the magnitude of the fullerene potential has been studied in depth for a confined helium model [26]. In particular, the phenomenon of ‘mirror collapse’, where the wave functions interchange their characteristic probability distribution while keeping its position in the ordered list of eigenvalues and conserving its nodal structure. Without making an exhaustive description of the behavior of the states around each crossing, we want to show that the same kind of phenomena presents here the endohedrally confined hydrogen atom with a moving nucleus. This time we also show what happens when we vary the mass of the fullerene cage while keeping the magnitude of the C_{60} potential fixed.

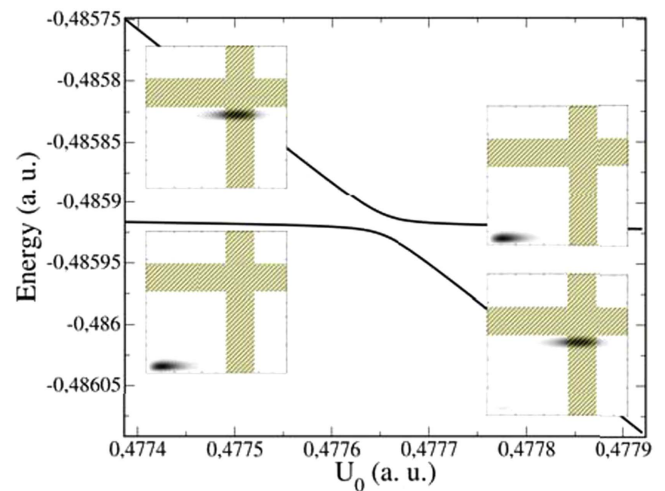


Figure 4. Mirror collapse between the first two states of the confined H system for the evolution of the energy values as a function of the potential U_0 . Inner boxes show the spatial distribution of the two states at the left and right sides of the crossing (the abscissa corresponds to the electron radial coordinate and the ordinate to the proton one), where it can be seen that the spatial distribution of the particles becomes interchanged.

Figure 3 shows the evolution of the negative energy levels as a function of U_0 . We see that the ground state energy is not equal to -0.5 , but higher. In this case we use $20Sf_b$ per radial coordinate and $l_{\max} = 2$. This is because of the confinement and also the finite size of the partial wave and radial expansions. Although the energy values are not too precise with these basis dimensions, the results are representative enough for the understanding of the phenomena we want to describe.

We can observe an avoided crossing between the first two energy levels as a function of U_0 , which occurs around $U_0 = 0.47$. In the inner box of figure 3, we see a magnification of this crossing, and at figure 4 the density plots of the two-dimensional probability distributions for both states at the left and right of the crossing, where the interchange of probabilities occurring is clearly shown. In this case, the ground-state behavior corresponds to the atom centered at the cage in a typical ‘free’ hydrogen distribution, while in the first excited state the bounded pair is located close to the surface, with the proton and the electron within and inside the C_{60} potential, respectively.

To understand this behavior, we have to note that for small values of U_0 the ground state has practically no overlap with the fullerene well, so its energy does not depend on U_0 . The first excited state corresponds to the case where the electron lies in the well and the proton is around it. Again, localization of the proton is less expensive from a kinetic energy point of view, and it tends to locate as close to the electron as possible, without overlapping the repulsive region. The energy of the first excited state linearly decreases with U_0 at 0.45, and at $U_0 = 0.47$ it encounters the ground-state energy. At the same time, the ground state pair starts to move to the well gradually since its configuration there has the same energy as at the center of the cage. As the states become

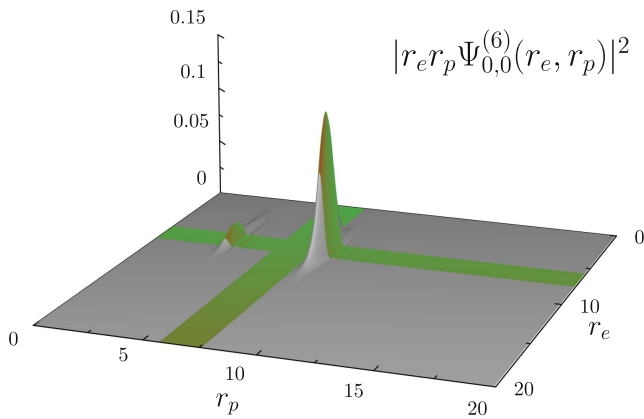


Figure 5. Three-dimensional plot for the 4th excited state of the confined hydrogen atom, of energy -0.573 for $U_0 = 0.575$. Distribution shows the proton localized outside the fullerene structure.

quasi-degenerate, their nodal structure is maintained, with the ground state never having nodal surfaces. The crossing is ‘avoided’, i.e. the states never have exactly the same energy value for a fixed U_0 .

A striking distribution appears for $U_0 \neq 0$, and corresponds to a bound state where the proton is mostly outside the fullerene. The distribution mixes through the crossing structure of figure 3 and is amplified in the upper inner box. It corresponds to the 4th and 5th excited states, having an energy close to -0.573 (lower than the hydrogen bound state). In figure 5, the spatial distribution for the 4th state is shown and is related to a bound state of the system in which the proton distribution is *outside* the fullerene cage. Crossing appears close to $U_0 = 0.575$ and is shown in figure 3. Note that, asymptotically, the field in which the proton moves is Coulombic. As is known for potentials with asymptotic Coulomb tails [28], there exists an infinite number of bound states. We estimate that there exists an infinite number of states with these characteristics for the proton distribution (i.e. located outside the fullerene cage).

Finally, we vary the mass of the fullerene molecule in search of crossings, from (nonphysical) values $\simeq 1$ a.u. to 1.44×10^6 a.u. (the order of magnitude of the exact value for fullerene molecule). We found that all the crossings occur at mass values which are small compared to the mass of the C_{60} fullerene or other species C_n . However, we found a situation we think is interesting to describe, and which could be present in confinement of heavier atoms or molecules. Figure 6 shows the crossing between the 5th and 6th energy levels when m_3 varies from 660 to 770 m_e .

In this particular case, the localization of the particles (shown in the inner boxes) also becomes interchanged and corresponds to the case where the atom localizes inside the C_{60} potential. The distribution of both states represents very different situations for the proton distribution, one where the proton has an oscillating inner distribution in the region $r_p \lesssim 4$, and the other glued to the fullerene surface from the inner side ($4 \lesssim r_p \lesssim 6$).

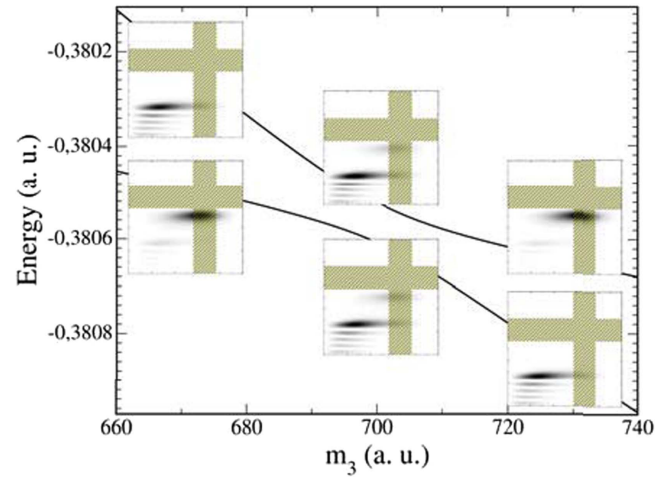


Figure 6. Mirror collapse between the two first states of the confined H system for the evolution of the energy values as a function of the fullerene mass m_3 . Their properties become interchanged when the C_{60} mass varies from 660 to 740 electron mass.

4. Conclusions

We have studied the confinement of the hydrogen atom in a spherical cavity through a quantum mechanical model which considers both electron and proton dynamics. We have considered the case of a spherical well of impenetrable walls and a fullerene, C_{60} , which was modeled as a spherical barrier, attractive for the electron and repulsive for the proton. The dynamics were driven by the solutions of the three-body-like Schrödinger equation, where the motion of the particles is described in the coordinates which locate them with respect to the center of the spherical cavity. The solution was obtained by using the generalized Sturmian functions method.

The wave functions showed behavior that differs substantially from the many models found in the literature, where the proton is fixed at the center of the coordinate system, or moves perturbatively in the Born–Oppenheimer approximation. In the moving nucleus case, the states showed a different proton distribution for each energy level, being the bound state with the proton located outside the fullerene, one of the more curious situations which manifested the complexity of the system. For a fullerene potential which was deep enough to keep the electron bounded at least in one state, we can argue that the asymptotic interaction for the proton corresponded to an attractive Coulombic tail, which supported infinitely many bound states [28], in particular Rydberg states.

The spectrum of the system in the moving nucleus case was much more dense than that given for the fixed nucleus. The ‘new’ levels were associated with the dynamics of the proton, and can be understood by considering the distance between the energies for a confined particle decreasing with the inverse of the mass.

Apart from the complexity of the moving nucleus system, we found one match with the fixed nucleus model for the ground state of weak fullerene wells. In that case, the proton located at the center of the molecule, and the same happened

for the rigid sphere. The corresponding distribution of the center of mass of the atom was very different to the box ground state of a neutral particle. It reflected how different the dynamics of a simplified model could be from a composite system.

Finally, we found crossing phenomena for the spectrum as a function of the parameters of the equation. By varying the magnitude of the fullerene well, we found many avoided crossings, while by changing the fullerene mass, we found only one. These are the preliminary results of a more exhaustive search for crossings which will include the variation of radius of the fullerene well. This change of radius would actually happen if the vibrational modes of the carbon structure were considered. The results will be part of an forthcoming publication.

Acknowledgments

This work has been supported by ANPCyT (PICT-2014-1400) and CONICET (Argentina). J M R thanks the support of Universidad Nacional de Cuyo through grant 06/624.

References

- [1] Ehrhardt H, Schulz M, Tekaas T and Willmann K 1969 *Phys. Rev. Lett.* **22** 89
- [2] Shah M B and Gilbody H B 1981 *J. Phys. B: At. Mol. Phys.* **14** 2361
- [3] Kerby G W, Gealy M W, Hsu Y-Y, Rudd M E, Schultz D R and Reinhold C O 1995 *Phys. Rev. A* **51** 2256
- [4] Beynon J D E 1965 *Nature* **207** 405
- [5] Bergeman T *et al* 1984 *Phys. Rev. Lett.* **53** 775
- [6] Komatsu K, Murata M and Murata Y 2005 *Science* **307** 238
- [7] López-Gejo J, Martí A A, Ruzzi M, Jockusch S, Komatsu K, Tanabe F, Murata Y and Turro N J 2007 *J. Am. Chem. Soc.* **129** 14554
- [8] Cohen-Tannoudji C, Diu B and Laloe F 2006 *Quantum Mechanics* (Hoboken, NJ: Wiley-Interscience)
- [9] Amusia M Y, Liverts E Z and Mandelzweig V B 2006 *Phys. Rev. A* **74** 042712
- [10] Bielinska-Waz D, Karwowski J and Diercksen G H F 2001 *J. Phys. B: At. Mol. Opt. Phys.* **34** 1987
- [11] Rivelino R and Vianna J D M 2001 *J. Phys. B: At. Mol. Opt. Phys.* **34** L645
- [12] Saha B, Mukherjee T K, Mukherjee P K and Diercksen G H F 2002 *Theor. Chem. Acc.* **108** 305
- [13] Neek-Amal M, Tayebirad G and Asgari R 2007 *J. Phys. B: At. Mol. Opt. Phys.* **40** 1509
- [14] Ferreyra J M and Proetto C R 2013 *Am. J. Phys.* **81** 860
- [15] Tanner A C 1991 *Am. J. Phys.* **59** 333
- [16] Amore P and Fernández F M 2010 *Eur. J. Phys.* **31** 69
- [17] Sech C L and Banerjee A 2011 *J. Phys. B: At. Mol. Opt. Phys.* **44** 105003
- [18] Connerade J P, Dolmatov V K, Lakshmi P A and Manson S T 1999 *J. Phys. B: At. Mol. Opt. Phys.* **32** L239
- [19] Ferreyra J M and Proetto C R 1995 *Phys. Rev. B* **52** R2309
- [20] Fernández F M 2010 *Eur. J. Phys.* **31** 285
- [21] Fernández F M, Aquino N and Flores-Riveros A 2012 *Int. J. Quantum Chem.* **112** 823
- [22] Xu Y B, Tan M Q and Becker U 1996 *Phys. Rev. Lett.* **76** 3538
- [23] Randazzo J M, Ancarani L U, Gasaneo G, Frapiccini A L and Colavecchia F D 2010 *Phys. Rev. A* **81** 042520
- [24] LAPACK—Linear Algebra PACKage, <http://netlib.org/lapack/>
- [25] Kato D and Watanabe S 1995 *Phys. Rev. Lett.* **74** 2443
- [26] Mitnik D M, Randazzo J and Gasaneo G 2008 *Phys. Rev. A* **78** 062501
- [27] Aquino N, Flores-Riveros A and Rivas-Silva J F 2003 *Phys. Lett. A* **307** 326
- [28] Ma Z-Q 1986 *Phys. Rev. D* **33** 1745